DOI: 10.13009/EUCASS2019-811

Numerical modelling of mechanical behaviour of weft-knitted carbon fiber composites

M. Ravandi, S. Ahlquist*,**, M. Banu**
**Department of Mechanical Engineering, University of Michigan*
2350 Hayward St, Ann Arbor, MI 48109, USA, mbanu@umich.edu
***Taubman School of Architecture, University of Michigan*
2000 Bonisteel Boulevard, Ann Arbor, MI 48109, USA

Abstract

Knitted textiles as a reinforcement in polymer composites are popular for high drape properties and superior impact energy absorption, which makes them suitable for certain composite components. However, since knitted textiles usually offer lower stiffness and strength, limited attention has been given to the modeling of mechanical behavior of knitted fabric composites. In this study, a 3D finite element (FE) modeling of a precise geometrical model of weft-knitted carbon fiber thermoplastic composite is presented to study the material behavior and damage mechanisms. A continuum damage mechanics (CDM) approach and cohesive zone model is applied to model the matrix damage and yarn/matrix debonding, respectively. It is found that the interfacial strength can have a significant effect on the tensile performance of the knitted fabric composites, particularly when they are subjected to a large strain.

1. Introduction

Complex geometry structures used in space applications such as self-deployable systems require specific properties such as high thermal and impact resistance as well as high flexibility of the structure. Currently, woven/unwoven carbon fiber textiles used for reinforcing the composites offer promising mechanical properties, however, they are inflexible due to their two-dimensional (2D) structure of the reinforcements which gives the high performance of the mechanical properties only in the direction of the fibers. Knitted fabrics are an alternative textile to rigid reinforcements offering a capability for large 3-dimensional (3D) deformation [1–3]. Knitted fabrics can be employed as reinforcement in polymer composites and possess the potential to be produced by robotic textile manufacturing processes, which can introduce a new generation of functional material systems with tailored structural characteristics [4,5].

Knitted fabric refers to a class of textiles formed by inter-looping of yarns through particular needle motions. Comparing to the other textile processes, the knitting process results in a high degree of yarn curvature in the fabric architecture [6–8]. As a result, knitted fabrics generally offer lower mechanical properties compared to non-looped textiles where the loads are more or less uniformly distributed along the yarns. Moreover, they have a highly porous texture, resulting in a low fiber volume fraction when used as reinforcement [9]. However, knitted textiles own some unique advantages such as high drape properties and conformability, as well as high energy absorption characteristic, which make them an excellent reinforcement for composites with complex geometries [5,6].

Knitting process is traditionally divided into two general methods, warp knitting and weft knitting, and both methods are available to produce preforms using high-performance yarns, such as glass and carbon, for composite structures. To date, knitted composites have been utilized in the manufacture of a number of aircraft components such as wing panels, T-shape connectors, jet engine vanes, and I-beams [6,10,11]. However, unlike the other types of textile composites, knitted fabrics have not been frequently used in structural applications. Therefore, and due to the complexity of their geometric architecture compared to woven and braided fabrics, limited studies have been dedicated to capture mechanical and fracture behavior of knitted fabric composites and predict their elastic properties and strength.

In one of the first studies, Rudd et al. [12] developed a simple model based on the rule of mixtures to predict the stiffness of knitted glass fiber composite. The comparison of the predicted stiffness with the experimental data showed that the model requires modifications in order to take into account the fabric relaxation. In another study, Ramakrishna et al. [13] proposed an analytical model for predicting the in-plane mechanical properties of the knitted fabric laminates. The model integrated the effects of reinforcing yarns into the rule of mixture using a 2D geometrical model of the knitted fabric and neglected the effects of the out-of-plane yarns. This assumption led to a reasonable prediction of the

DOI: 10.13009/EUCASS2019-811

elastic modulus, however, there existed a significant discrepancy between the predicted and experimental tensile strength of the composites. A micromechanical approach using a 3D geometrical model of a plain weft-knitted fabric was proposed by Shekarchizadeh et al. [14] to derive the mechanical properties of the composite. They modeled a unit cell of a plain knitted fabric based on the geometrical model suggested by Vassiliadis et al [15], then conducted a finite element (FE) simulation to extract the elastic properties of the composite. However, more precise geometrical models of knitted fabrics are necessary in order to enhance the accuracy of the virtual tensile test to predict the performance of knitted composites. In order to capture the force-determined geometry and residual stresses imposed during the knitting process, Duhovic et al. [8] conduct a dynamic finite element simulation of the manufacturing process. Then, the resultant geometry was used in an FE modeling of the knitted fabric composite to investigate the mechanical performance.

Many geometrical modeling strategies have been suggested for capturing the geometry of different types of textiles, such as 2D-3D woven, braided, and knitted [5,9,16–20]. These geometries were used for micro-scale and multiscale models to estimate elastic properties and predict the fracture behavior of these textile composites. Among others, polynomial splines are more suitable to represent the curve of a knitted loop [20,21]. Liu et al. [21] carried out a 3D finite element analysis of the weft-knitted fabric in order to investigate the effects of the material architecture on both in- and out-of-plane displacements. However, the assessment of the effects of these deformations on the mechanical behavior of the knitted fabric composites is still lacking.

The mechanical behavior and strength of a composite not only depend on the properties of its constituent (i.e. fiber and matrix) but also the properties of the interfaces. In general, fiber/matrix interface failure is one of the main failure modes in composites which can deteriorate their load carrying capacity. Unlike the other types of textile composites, the influence of fiber/matrix (inter-yarn) and yarn/matrix (intera-yarn) failures in knitted composites is not well investigated in the literature [7].

This study aims to numerically investigate the mechanical performance of the weft-knitted carbon fiber thermoplastic composite through a direct simulation based on 3D finite element analysis. The finite element model includes the yarn, matrix, and yarn/matrix interactions. Based on this model, a simulation strategy is proposed which is able to capture the large-strain non-linear material response of weft-knitted composites. A proper numerical model to predict the mechanical behavior of weft-knitted composites not only provide a valuable insight into how damage propagation is affected by the fabric architecture but also can help to calibrate macroscopic properties.

2. Simulation Framework

2.1 Geometrical Modelling

There are a variety of types of knitted fabrics which are categorized into two main classifications, known as weft- and warp-knitted fabrics. Weft-knitted fabrics, which are generally produced by interlacing one yarn, are the most common and cost-effective knitted fabrics. The plain weft-knitted fabric, known as “single jersey”, was used in this study. The knitting pattern and the main geometrical parameters of a plain weft-knitted fabric are illustrated in Figure 1. The horizontal and vertical row of loops in knitted fabrics are known as course and wale, respectively.

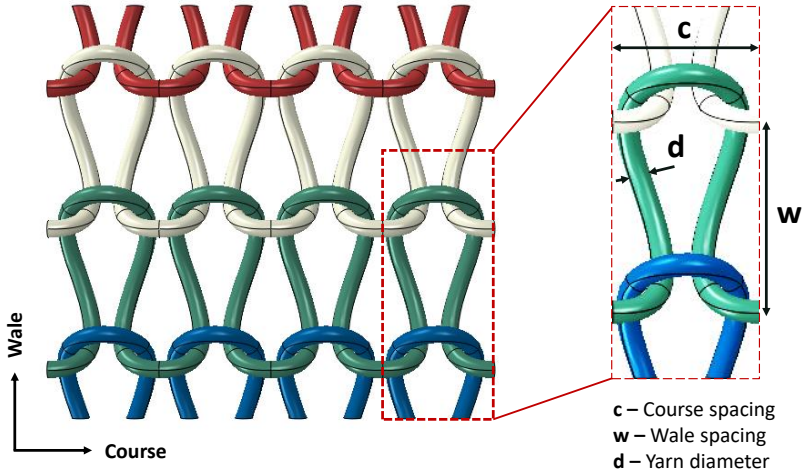

Figure 1: Knitting pattern of the plain weft-knitted fabric and its geometrical parameters.

DOI: 10.13009/EUCASS2019-811

The 3D geometry of the plain knitted loop was created by sweeping the circular cross-section of the yarn along the spatial curve defining the centerline path of the yarn. The yarn centerline of a periodic knitted loop was defined using a B-spline curve passing through a set of 9 points (i.e. $\{P_1, \dots, P_9\}$), as shown in Figure 2a [20]. Due to the periodic structure, the centerline curve was defined so that the first and second derivatives remain continuous along the connected loops. The x, y, z coordinates of the points P_1 to P_9 shown in Figure 2a are calculated based on the actual geometrical parameters of the knitted fabric, i.e. course (row) spacing and wale (column) spacing of loops, and yarn diameter. The coordinates of these points in terms of the fabric parameters are given in Eq.(1). The values of the geometrical parameters used in this study were obtained from the experimental specimen shown in Figure 2b.

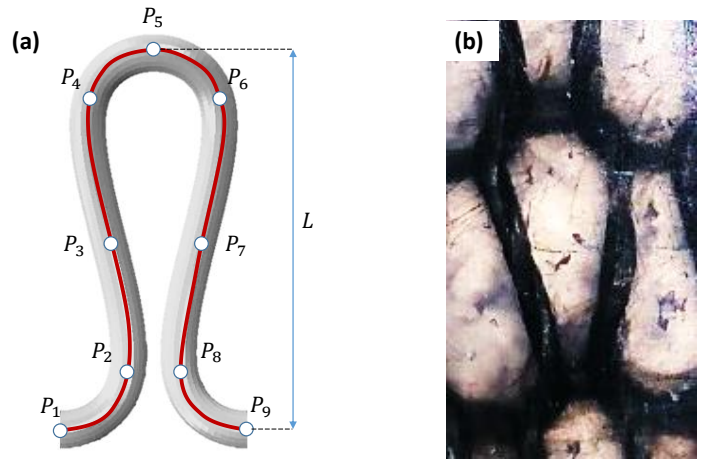

Figure 2: (a) Schematic illustration of the yarn centerline curve of a knitted loop and the points (P_1-P_9) used to define the B-spline curve, (b) the single jersey knitted carbon fiber/PP composite specimen.

$$
\begin{aligned}
P_1 &= \left(0,0,\frac{d}{2}\right) & P_6 &= \left(\frac{3c+2d}{4},\frac{L+w}{2},0\right)\\
P_2 &= \left(\frac{c+2d}{4},\frac{L-w}{2},0\right) & P_7 &= \left(\frac{3c}{4},\frac{L}{2},-\frac{d}{2}\right)\\
P_3 &= \left(\frac{c}{4},\frac{L}{2},-\frac{d}{2}\right) & P_8 &= \left(\frac{3c-2d}{4},\frac{L-w}{2},0\right)\\
P_4 &= \left(\frac{c-2d}{4},\frac{L+w}{2},0\right) & P_9 &= \left(c,0,\frac{d}{2}\right)\\
P_5 &= \left(\frac{c}{2},L,\frac{d}{2}\right)
\end{aligned}
\qquad \textbf{(1)}
$$

where c, d, and w were defined in Figure 1. L is the height of the knitted loop as shown in Figure 2a.

2.2 Periodic boundary conditions

The FE analysis of a periodic representative volume element (RVE) is a useful technique to study the material properties and estimate the effective properties of composites. In order to ensure that the assembly of RVEs always satisfies the compatibility conditions, periodic boundary conditions (PBCs) must be applied. The PBCs guarantee the continuity of the displacement and traction field for the adjacent RVEs. Applying the periodic displacement boundary conditions, the latter condition can be automatically satisfied in the displacement-based analysis [22]. The periodic displacement boundary conditions were imposed using the linear constraint of Eq.(2) between each pair of corresponding nodes on the opposite surfaces of the RVE:

$$u_i^{j+} - u_i^{j-} = \bar{\varepsilon}_{ik}\left(X_k^{j+} - X_k^{j-}\right), i = x, y, z \qquad \textbf{(2)}$$

DOI: 10.13009/EUCASS2019-811

where u and X indicate the displacement and coordinate of nodes, respectively, "$j+$" and "$j-$" denote the jth pair of opposite nodes on RVE boundaries, and $\bar{\varepsilon}_{ik}$ and is the global strain of the RVE. A python script was developed to implement the PBCs.

2.3 Material Model

A mesoscale 3D finite element (FE) model of a representative volume element (RVE) of the plain knitted fabric composite, was created and analyzed using the commercial software Abaqus/Explicit. The geometrical model of the fabric with the assumption of a circular cross-sectional fiber tow was created based on the approach described in the previous section. The pure matrix block was constructed by cutting out the geometry of the modeled fabric from a complete rectangular block. The fiber tow and the pure matrix were modeled using an 8-node brick element (C3D8R) and a 4-node tetrahedral element (C3D10M), respectively. The complete RVE model of the knitted composite and its constituting components are shown in Figure 3a. The fiber volume fraction (V_f) – the ratio of fiber volume to the entire volume – of the RVE is calculated to be 10.5%.

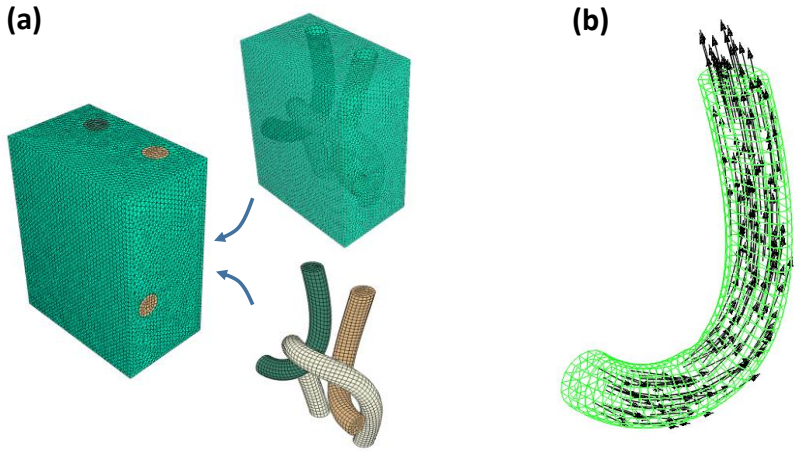

Figure 3: (a) 3D RVE model of the knitted composite, (b) FE model of a yarn with local material orientation vectors (note: only fiber direction is shown).

An isotropic elastic-plastic material model was used to model the nonlinear constitutive response of the pure matrix. The yarn was assumed to be fully impregnated with the matrix resin as a unidirectional composite. Thus, an orthotropic constitutive law with material properties of a unidirectional carbon fiber/PP composite was used to describe the behavior of the fiber tow. Due to the anisotropy of the fiber tow and its curved shape, it is important to ensure that the stress and strain components are defined correctly along the material orientation for each element. Since the yarn cross-section meshes are linked together along the yarn centerline (i.e. fiber direction), the local material orientation of each element can be obtained from the vector linking the center of the bottom to the top face of the element [23]. A python script was written to calculate the local material orientations based on the nodal coordinates of elements. Abaqus Discrete Field was used to define the material orientation of elements (Figure 3b).

2.4 Interface

The yarn/matrix debonding in knitted fabric composites is a complex failure mode which occurs outside the yarn at the interface with the surrounding matrix. The yarn/matrix interface was modeled using the cohesive zone model (CZM) with a bilinear traction-separation law. The Abaqus surface to surface contact algorithm with a cohesive behavior was used to define the interaction between the yarn and matrix. The interface failure onset was modeled using the quadratic failure criterion [24,25]. The interface damage evolution was specified based on the fracture energy criterion. The mixed-mode fracture energy was determined by the Benzeggagh and Kenane (B-K) relation [26]. Once the interface fails, the stresses are transmitted by means of a hard contact algorithm with a tangential friction coefficient of 0.001. The same algorithm was used for the yarn/yarn interaction.
The material properties used in the modeling of the carbon fiber knitted composite are summarized in Table 1.

DOI: 10.13009/EUCASS2019-811

Table 1: Material properties used in numerical modeling.

Yarn properties	$E_1 = 236.79$ GPa; $E_2 = E_3 = 10.260$ GPa; $G_{12} = G_{13} = G_{23} = 7.17$ GPa; $v_{12} = 0.26$; $v_{13} = v_{23} = 0.3$
Resin properties	$E_1 = 4.018$ GPa; $v_{12} = 0.3$; $\tilde{\sigma}_{y0} = 23.9$ MPa;
CZM properties	$G_{IC} = 0.15$ KJ/m^2; $G_{IIC} = G_{IIIC} = 0.2$ KJ/m^2; $\eta = 1$; $\sigma_{\mathrm{I}}^{\mathrm{C}} = 25$ Mpa; $\sigma_{\mathrm{II}}^{\mathrm{C}} = \sigma_{\mathrm{III}}^{\mathrm{C}} = 50$ Mpa

3. Results & discussion

The stress-strain curves of the numerical simulation of the weft-knitted carbon fiber/PP composite in the wale and course directions are shown in Figure 4. The results are also compared with pure matrix response in order to evaluate the in-plane performance of the composite of knitted fabric with a V_f of 10%. According to the figure, the wale direction yields higher tensile properties compared to the course direction. The initial elastic modulus along the wale direction is 19% higher than that of along the course direction. This is attributed to the larger wale spacing in this knitted fabric structure (Figure 1), which leads to stretching the yarn and consequently having more fibers aligned in the wale direction.

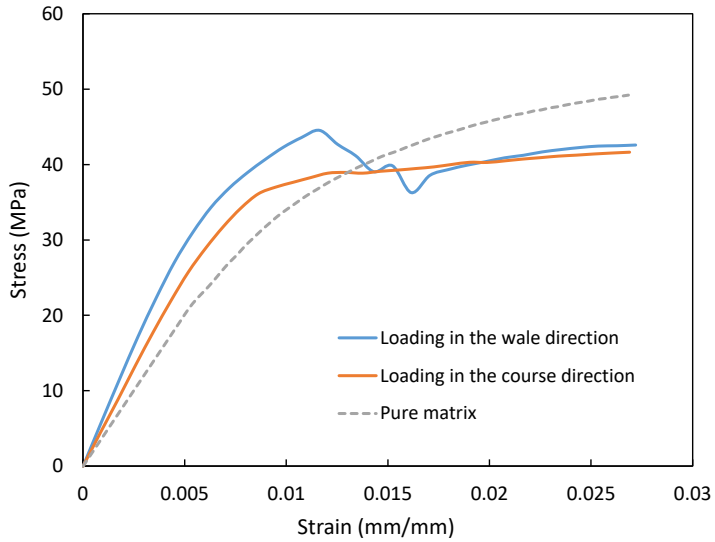

Figure 4: Stress-strain response of RVE model of weft-knitted carbon fiber/PP composite and pure matrix.

When comparing to the unreinforced polymer (i.e. pure matrix), the stress-strain curves can be considered in two regions, i.e. the linear elastic region and the nonlinear plastic region. In the first region, the tensile performance of the knitted composite is superior and has a higher elastic modulus in both the wale and course directions. However, the load-bearing capacity of the composite drops below the pure matrix in the plastic region. Moreover, the tensile response of the composite in the wale direction shows a clear stress drop in the plastic region. This behavior of stress is clearly attributed to the debonding occurred at the yarn/matrix interface during tension as the cohesive failure at the yarn/matrix interface is the only failure mechanism that can be captured by this model. Hence, it can be said that the effect of the interfacial failure in the knitted fabric composites is not negligible and has to be taken into account for high-fidelity modeling. This is discussed more in the next section.

In order to determine the effect of debonding at the yarn/matrix interface on the tensile performance of the composite, the cohesive interaction was replaced by “Tie Constrain” algorithm in the simulation of RVE. In this algorithm, the yarn surfaces are tied to the neighboring surfaces on the matrix by sharing nodes. Figure 5 shows the effect of the

DOI: 10.13009/EUCASS2019-811

yarn/matrix interface failure on the stress-strain curves in both the principle directions. It can be observed that, in both the directions, the initial linear elastic behavior is identical for both the tie constraint and the cohesive interaction. However, with the initiation of cohesive failure at yarn/matrix interface, the stress-strain curves of the model with cohesive interaction show higher nonlinearity and begin deviating from the results of the model with no failure assumption. When comparing to the response of pure matrix, the influence of debonding at yarn/matrix interfaces can lower the performance of the composite even below the pure matrix in the plastic region. Conversely, in the case of no debonding (i.e. tie constraint), the stress-strain response of the knitted composite is always superior to the unreinforced polymer. Hence, due to the fact that the knitted composites are often recommended for applications with large deformations, the effect of the interfacial failure has to be considered in modeling of these composites.

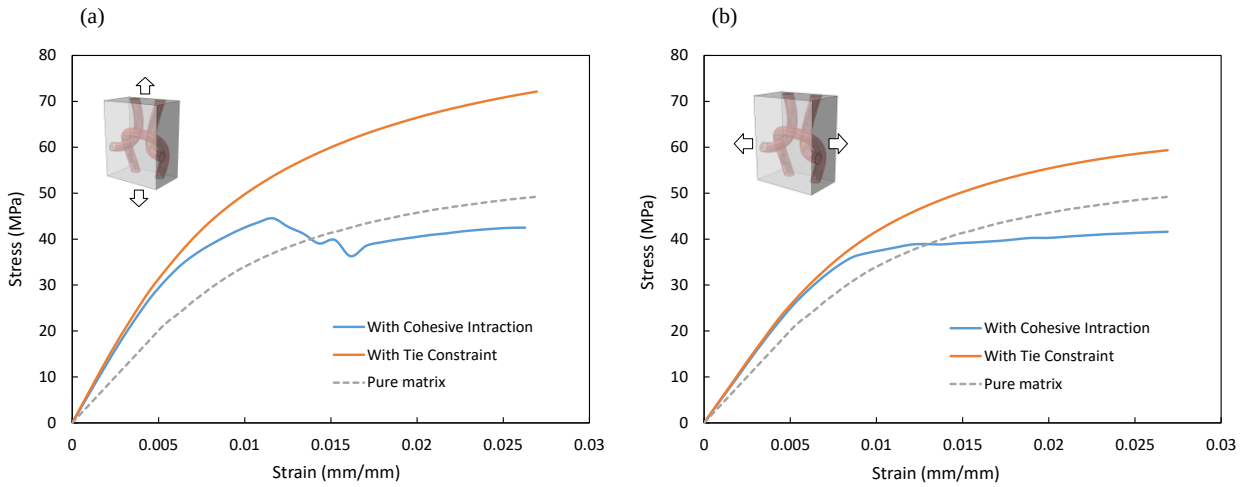

Figure 5: Effect of yarn/matrix debonding on the tensile performance of the composite.

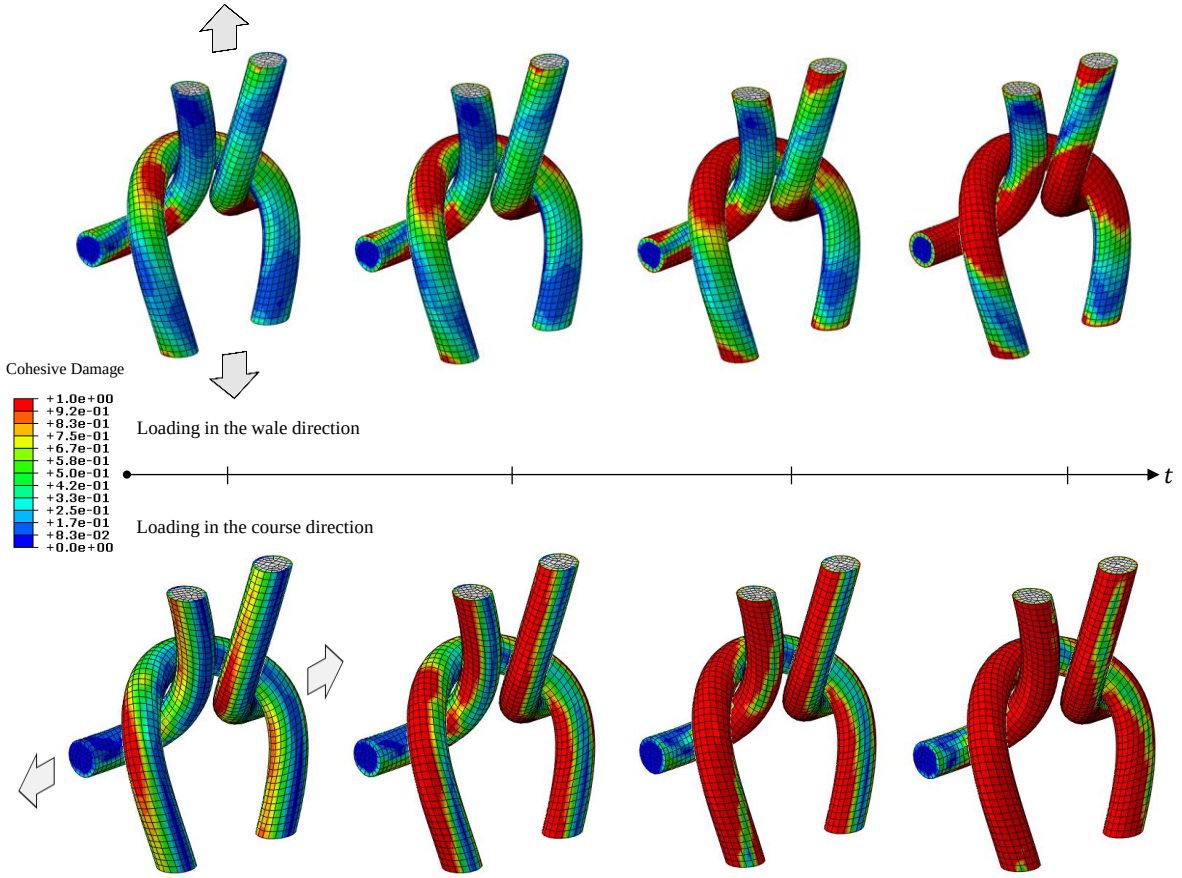

Figure 6: Cohesive damage evolution at the yarn/matrix interfaces of the knitted composite RVE during tension in the principle directions.

DOI: 10.13009/EUCASS2019-811

Figure 6 illustrates the cohesive damage evolution on the yarns' surfaces of the knitted composite during tension along the wale and course directions, at four different time-steps. It can be observed that for the loading in the wale direction, the cohesive damage forms and propagates on the horizontal part of the yarns – perpendicular to the loading direction, till debonding occurs all over the yarns. In contrast, the formation of the cohesive damage is on the vertical surfaces of the yarns when loaded in the course direction. It is evident from this figure that the cohesive damage, i.e. yarn/matrix debonding, is an extensive damage in the knitted composite. This behavior is mainly due to the complexity of the knitted fabric structure, which enables the yarn to move and rotate extensively during tension or compression.
The energy dissipated by the yarn/matrix debonding (i.e. cohesive damage) and matrix plasticity are compared with the elastic strain energy in Figure 7 as a function of strain. The cohesive damage, plasticity and elastic strain energy are the main energy absorption mechanisms as their summation are almost equal to the total internal energy of the RVE. Figure 7 indicates that the energy dissipated by matrix plasticity during tension is significantly higher than the energy dissipated by the cohesive damage for both loading cases. The energy dissipated by cohesive damage is 7.8% and 9% of the total internal energy of the RVE loaded in the wale and course direction, respectively, whereas the contribution of matrix plasticity is almost 61.3% and 59.4%. The rest of the internal energy is a recoverable energy corresponding to the elastic strain energy. The large plastic dissipation energy is related to the low fiber volume fraction ($V_f = 10\%$) and the complexity of the knitted fabric structure, which leads to complex deformation of the matrix. Consequently, the energy absorbed by matrix, which is composed of elastic energy and plastic dissipation, is the main energy absorption mechanisms.

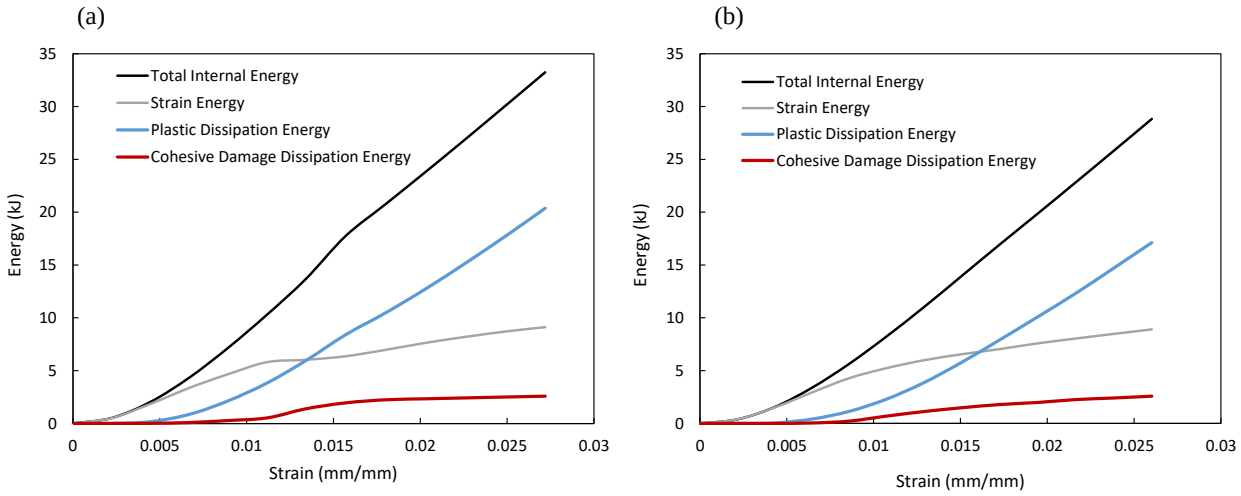

Figure 7: Comparison of energy dissipated by cohesive damage and plasticity of matrix with elastic strain energy for (a) loading in the wale direction and (b) loading in the course direction.

4. Conclusions

In this study, a 3D finite element simulation framework was presented to study the tensile behavior and damage mechanisms of the weft-knitted carbon fiber thermoplastic. The procedure of creating a precise geometrical model of the knitted fabric composite was provided. A representative volume element (RVE) of the knitted composite was used for finite element analysis by applying periodic boundary conditions. The interaction between yarn surfaces and surrounded matrix was molded using two different algorithms, namely cohesive interaction and tie constraint, in order to assess the effects of yarn/matrix debonding on the tensile behavior of the composite. According to the simulation results, the tensile performance of the weft-knitted composite in the wale direction always was superior. The results showed that the weft-knitted fabric reinforcement can improve the elastic modulus of the polymer by at least 27% at a fiber volume fraction as low as 10%. It was also shown that, regardless of the types of yarn/matrix interaction, the initial elastic modulus of the composite in the wale direction is 19% higher than that of in the course direction. Comparing the results of the two different interaction algorithms showed that debonding at the interface between the outer surface of yarn and the matrix can have a significant effect on the tensile performance of the knitted composites. It is therefore essential to consider the effect of interfacial failure in the FE simulation of knitted composites to achieve a more accurate prediction of their mechanical behavior.

DOI: 10.13009/EUCASS2019-811

References

[1] Hasani H, S. Hassanzadeh, MJ. Abghary, E. Omrani. 2017. Biaxial weft-knitted fabrics as composite reinforcements: A review. *J. Ind. Text*. 46:1439–73

[2] Omrani E, H. Hasani, F. Esmaeili. 2018. Mechanical performance of tubular composites reinforced by innovative 3D integrated knitted spacer fabrics. *J. Appl. Polym. Sci*. 135:46074.

[3] Takano N, M. Zako, R. Fujitsu, K. Nishiyabu. 2004. Study on large deformation characteristics of knitted fabric reinforced thermoplastic composites at forming temperature by digital image-based strain measurement technique. *Compos Sci Technol*. 64:2153–63.

[4] Sabantina L, F. Kinzel, A. Ehrmann, K. Finsterbusch. 2015. Combining 3D printed forms with textile structures - mechanical and geometrical properties of multi-material systems. *IOP Conf Ser: Mater Sci Eng*.87:012005.

[5] de Araújo M, R. Fangueiro, H. Hong. 2004. Modelling and simulation of the mechanical behaviour of weft-knitted fabrics for technical applications. *AUTEX Research Journal*. 1:4-9.

[6] Tong L, Mouritz AP, Bannister MK. 2002. 3D Fibre Reinforced Polymer Composites. Elsevier Science, Oxford.

[7] Huysmans G, I. Verpoest, P. Van Houtte. 2001. A damage model for knitted fabric composites. *Compos Part A Appl Sci Manuf.* 32:1465–75.

[8] Duhovic M, D. Bhattacharyya. 2006. Simulating the deformation mechanisms of knitted fabric composites. *Compos Part A Appl Sci Manuf*.37:1897–915.

[9] Siddiqui MK, D. Sun. 2015. Porosity prediction of plain weft knitted fabrics. *Fibers*. 3:1-11

[10] Low H, P. Greaves, J. King. 1998. Composite materials in aero gas turbines: performance potential versus commercial constraint. Aircraft Eng & Aerospace Tech.70:3.

[11] Paul R. 2019. High Performance Technical Textiles. John Wiley & Sons.

[12] Rudd CD, MJ. Owen, V. Middleton. 1990. Mechanical properties of weft knit glass fibre/polyester laminates. *Compos Sci Technol*.39:261–77.

[13] Ramakrishna S. 1997. Characterization and modeling of the tensile properties of plain weft-knit fabric-reinforced composites. *Compos Sci Technol*. 57:1–22.

[14] Shekarchizadeh N, MM. Abedi, R. Jafari Nedoushan. 2016. Prediction of elastic behavior of plain weft-knitted composites. *J Reinf Plast Comp*. 35:1613–22.

[15] Vassiliadis SG, CG. Provatidis, AE. Kallivretaki. 2007. Mechanical simulation of the plain weft knitted fabrics. *Int Jnl of Clothing Sci & Tech.* 19:109–30.

[16] Kurbak A, O. Ekmen. 2008. Basic Studies for Modeling Complex Weft Knitted Fabric Structures Part I: A Geometrical Model for Widthwise Curlings of Plain Knitted Fabrics. *Text. Res. J*. 78:198–208.

[17] Xu L, CZ. Jin, SK. Ha. 2015. Ultimate strength prediction of braided textile composites using a multi-scale approach. *J. Compos. Mater*. 49:477–94.

[18] Ansar M, W. Xinwei, Z. Chouwei. 2011. Modeling strategies of 3D woven composites: A review. *Compos Struct*. 93:1947–63.

[19] Xu L, Y. Huang, C. Zhao, SK. Ha. 2016. Progressive failure prediction of woven fabric composites using a multi-scale approach. *Int. J. Damage Mech*. *27*(1), 97–119.

[20] Siddiqui MK. 2014. Geometrical Modelling and Numerical Analysis of Thermal Behaviour of Textile Structures. PhD Thesis. Heriot-Watt University, School of Textiles and Design.

[21] Liu D, D. Christe, B. Shakibajahromi, C. Knittel, N. Castaneda, D. Breen, et al. 2017. On the role of material architecture in the mechanical behavior of knitted textiles. *Int J Solids Struct*. 109:101–11.

[22] Xia Z, C. Zhou, Q. Yong, X. Wang. 2006. On selection of repeated unit cell model and application of unified periodic boundary conditions in micro-mechanical analysis of composites. *Int J Solids Struct*. 43:266–78.

[23] Sherburn M. 2007. Geometric and mechanical modelling of textiles. PhD Thesis. University of Nottingham.

[24] Camanho PP, CG. Dávila. 2002. Mixed-mode decohesion finite elements for the simulation of delamination in composite materials. NASA-Technical Paper. 211737:33.

[25] Ravandi M, U. Kureemun, M. Banu,W. Teo, L. Tong, TE. Tay, et al. 2019. Effect of interlayer carbon fiber dispersion on the low-velocity impact performance of woven flax-carbon hybrid composites. *J. Compos. Mater*. *53*(12), 1717–1734.

[26] Benzeggagh ML, M. Kenane. 1996. Measurement of mixed-mode delamination fracture toughness of unidirectional glass/epoxy composites with mixed-mode bending apparatus. *Compos Sci Technol*. 56:439–49.